4ICEGE Thessaloniki-GREECE 2007

4th International Conference on
Earthquake Geotechnical Engineering
June 25-28, 2007
Paper No. 1152

UNCOUPLED NUMERICAL ANALYSIS FOR GROUND LATERAL SPREAD EFFECTS ON SINGLE PILE

San-Shyan LIN [1], Yu-Ju TSENG [2], Jen-Cheng LIAO[3], C.H. WANG[4], and Wei F. LEE[5]

ABSTRACT

Permanent ground deformation or ground lateral spreading is observed to be the main cause for distress of piles embedded in liquefiable ground. The purpose of this paper is to use uncoupled method to analyze ground lateral spread effect on piles. The computer code, CYCLIC-1D (Elgamal et al., 2002) developed at the University of California at San Diego and accessible from the web, is used for lateral ground deformation estimation. Subsequently, the pile performance, treated as beam on Winkler foundation, is studied based on the effect of ground deformation obtained from Cyclic-1D. Two centrifuge tested examples and one real field case were studied by the aforementioned method. Reasonable agreement was obtained between the predicted and measured results.

Keywords: Pile, Lateral Spreading, Soil Liquefaction

INTRODUCTION

It's known that the effects of liquefaction on piles are often damaging; the lateral spreading is usually triggered at the slightest inclined slope with liquefiable soils that are embedded in the soil layers. When the soil liquefaction was initiated, the liquefied soils tend to slide downward along the inclined surface. While the pile is embedded in these moving liquefied soils, the pile can sustain lateral force caused by the liquefied soils. Serious structural damages can be produced only when the upper part of the soils is liquefied, such as the 1964 Niigata earthquake (Hamada, 1992), the 1995 Kobe earthquake (Tokimatsu, 2003) and the 1999 Chi-Chi earthquake (Hwang et al., 2003), which had left extensive damage to many pile foundations of bridges and buildings.

Bhattacharya et al. (2004) proposed an alternative mechanism of pile failure in liquefiable deposits during earthquakes. It was considered that the pile becomes unstable under axial load from loss of support from the surrounding liquefied soil, provided the slenderness ratio of the pile in the unsupported zone exceeds a critical value. The instability causes the pile to buckle and cause a plastic hinge in the pile. In terms of soil pile interaction, the method assumes that, during instability, the pile pushes the soil. Hence, the lateral load effects are considered secondary to the basic requirement that piles in liquefiable soils must be checked against Euler's buckling. However, this method can only consider one plastic hinge instead of two plastic hinges, which are observed at the interfaces of the liquefiable soil layer sandwiched between two no-liquefiable soil layers.

[1] Professor, Department of Harbor and River Engineering, National Taiwan Ocean University, Taiwan, Email: sslin@mail.ntou.edu.tw
[2] Graduate Student, Department of Harbor and River Engineering, National Taiwan Ocean University, Taiwan, Email: nikilulu@gmail.com
[3] Assistant Researcher, Taiwan Construction Research Institute, Taiwan, Email: jeffrey.liao@yam.com
[4] Associate Researcher, Taiwan Construction Research Institute, Taiwan, Email: chwang@tcri.org.tw
[5] Researcher, Taiwan Construction Research Institute, Taiwan, Email: weilee@tcri.org.tw

Meyerhosn (1994) proposed that piles subject to lateral spreads resulting from soil liquefaction might cause two distinct failure modes. The first one is lateral pile deflections induced by ground lateral spreads that may result in the pile reaching its bending capacity and hence develops a plastic hinge. Another failure mode is the combined action of lack of sufficient lateral support due to the reduced stiffness of the liquefied soil and the lateral deflection imposed on the pile, which may result in pile buckling. Whether bending or buckling mode of a pile may develop depends primarily on the stiffness of the liquefied soil, length of pile exposed to liquefied soil, axial load imposed to pile, and bending stiffness of the pile. However, only bending failure analysis was conduced for the evaluated case histories.

Lin et al. (2005) back studied possible failure modes of three case histories. Whether these piles failed by either bending or buckling mode was re-evaluated. The design procedures suggested by Tokimatsu et al. (1998) and by JRA (1996) were also used for case histories evaluation and compared to available observation results. Two bending failure and one bulking failure among the three studied cases were concluded.

In order to understand the performance of the pile during soil liquefaction with the numerical analyses approach, the paper uses the uncoupled numerical analysis to resolve this problem. First, the Winkler type model is used to simulate the soil-structure interaction, and the Bouc-Wen model is used to mode soil behavior. At the same time, the Bouc-Wen model is also used to calculate the pile structure integrity while the pile fracture is triggered. Second, while considering the soil-structure interaction during soil liquefaction event, another important factor is the changing of the excessive pore water pressure. To obtain this solution, the CYCLIC-1D (developed at the University of California at San Diego) is used to generate the acceleration and excessive pore water pressure values within soils under the corresponded input earthquake motion. Then the values of excessive pore water pressures at various depths can be combined with the Winkler model.

In order to verify this uncoupled approach, this paper also simulates the results of two centrifuge tests and studies one real field case by the aforementioned method. Reasonable agreement was obtained between the predicted and the measured results.

MATERIALS MODELING

This study uses the Winkler model to simulate the soil-structure interaction caused by earthquake motion. Considering the force equilibrium between the surrounding soil and the pile itself, the equation is described as Eq. 1,

$$E_P I_P \frac{\partial^4}{\partial x^4} w(x,t) + m \frac{\partial^2}{\partial t^2} w(x,t) = F_S(x,t) + F_d(x,t) \tag{1}$$

where $w(x,t)$ = the lateral pile displacement in various time step t; x = depth to the ground surface; m = mass of pile; E_P = Young's Modulus of pile; I_P = moment of inertia of pile; $F_S(x,t)$ = non-linear soil reaction force; and $F_d(x,t)$ = radiating damping force of pile. Two major components of Eq. 1 are the $F_S(x,t)$ and $F_d(x,t)$. In the following, these two parts are defined based on the soil modeling.

After the initiation of soil liquefaction, the lateral force produced by the soil movement may cause an increasing bending moment. Furthermore, when the bending moment increases to a certain level, this may cause strength reduction in the material fracture. This study involves the pile fracture phenomenon that is described in the following section of moment-curvature relation of pile.

Soil Modeling

Based on the Bouc-Wen model, the force resulting from the nonlinear spring alone can be given as (Wen, 1985; Lin et al., 2002)

$$F_S(x) = \alpha \cdot K \cdot w + (1-\alpha) \cdot K \cdot w_0 \cdot \varsigma(x) \tag{2}$$

where α = a parameter controlling the post yielding stiffness; K = a reference stiffness; w = the pile deflection at the location of the spring; w_0 = the value of pile deflection that initiates yielding in the spring; and ς = a hysteretic dimensionless quantity.

The spring reactions of the pile for cohesion-less soils were given by Badoni and Makris (1996) as

$$F_s(x) = \mu \cdot \gamma_s \cdot d \cdot \frac{1+\sin\phi_s}{1-\sin\phi_s} \cdot x \cdot \zeta(x) \tag{3}$$

where d = the pile diameter; ϕ_s = the angle of the soil internal friction; μ = a parameter; and γ_s = the specific weight of the soil.

Another major concern of the soil liquefaction event is the initiation of the excessive pore water pressure. Kagawa et al. (1992) used a reduction factor F to describe the reducing soil strength as

$$F = (\sigma'/\sigma_0')^{\alpha} = (1-u)^{\alpha} \tag{4}$$

By combining Eq. 4 with Eq. 3, Eq. 5 shows the non-linear soil reaction force F_S with the effect of the reduction form the pore water pressure generation,

$$F_S = (1-u)^{\alpha}\ \mu\gamma_s d \frac{1+\sin\phi_s}{1-\sin\phi_s} x \cdot \zeta \tag{5}$$

When the soil-structure interaction is subjected to the seismic force, the radiation damping should be considered. According to Badoni and Makris (1996), it can be described as Eq. 6 and Eq. 7,

$$F_d = Q a_0^{-0.25} \rho_S V_S d\omega \langle \Delta w \rangle \tag{6}$$

$$Q = 2\left[1 + \frac{3.4}{\pi(1-\nu_s)}\right]^{1.25} \cdot \left(\frac{\pi}{4}\right)^{0.75} \tag{7}$$

where ν_s = Poison's ratio of soil; a_0 = non-dimensional frequency dependent parameter （ $a_0 = \frac{\omega d}{V_s}$ ）; ω = frequency; d = diameter of pile; V_s = shear velocity of soil; ρ_s = soil density; $\langle \Delta w \rangle = w_0 (\Delta w > w_0)$ for the non-linear case; and $\langle \Delta w \rangle = \Delta w (\Delta w \le w_0)$ for the linear case.

Under the effect of the excessive pore water pressure, Eq. 6 can be re-written as Eq. 8,

$$F_d = \left[(1-u)^{1/4} + \frac{V_L u}{(V_s + V_p)}\right] Q a_0^{-0.25} \rho_S V_S d\omega \langle \Delta w \rangle \tag{8}$$

where V_p = velocity of pressure; V_L = viscous velocity of liquefied soil.

Moment-Curvature Relation of Pile

The Bouc-Wen model is also used to model moment-curvature relationship of the pile and is expressed as (Lin et al., 2001)

$$M = \alpha\left(E_P I_P\right)\phi + (1-\alpha)M_y z \tag{9}$$

where M = the moment; M_y = the yield moment; ϕ = the curvature; α_M = a parameter controlling the rigidity of the pile after yielding; and z = the hysteretic parameter.

For concrete piles, once the moment induced on the pile exceeds a certain magnitude, the moment of inertia of the pile may be reduced due to concrete cracking. A semi-empirical moment versus moment of inertia relationship is used in this paper (Lin et al., 2001). The semi-empirical form is expressed as

$$I_{ef} = I^I,\ \left(M < M_{cr}\right) \tag{10}$$

$$I_{ef} = I^{II} + \left(I^I - I^{II}\right)\left(\frac{M_{cr}}{M}\right)^3,\left(M_{cr} < M < M_u\right) \tag{11}$$

where I_{ef} = the effective moment of inertia; $I^I = I_p$, the moment of inertia of the non-cracked section; I^{II} = the moment of inertia of the completely cracked section where the reinforcement has reached the yield strength; M_{cr} = the bending moment corresponding to the beginning of cracking; and M_u = the bending moment corresponding to I^{II}.

CENTRIFUGE TESTINGS

To verify the accuracy of the materials modeling proposed in this paper, the analytical results are compared with the measured data from the centrifuge testing results. Abdoun et al. (2003) presented the results of the centrifuge testing that simulates a single pile sustaining the lateral spreading force from the soil liquefaction. In this study, two centrifuge test cases are compared.

Case A

As shown in Fig. 1(a), the dimension of the box is 45.72m × 25.4m × 26.39m. The embedded model pile is 20cm long with diameter of 0.95cm; the soil material properties are shown in Table 1. This entire assemble is tested under a gravity value of 50g. Under such gravity, it can simulate a full-sized pile of 10m in length with 47.5cm in diameter. To test the soil liquefaction-induced lateral spreading effect, the layout of the model includes three layers of soils:

Top layer: 2m cemented sand with 34.5° of friction angle and 5.1kPa of cohesion.

Middle layer: 6m liquefiable sand (Nevada sand) with relative density of 40% and dry unit weight between 13.87 kN/m^3 and 17.33kN/m^3.

Bottom layer: 2m cemented sand with the same properties as the top layer.
(Note: the dimension shown above is the prototype model.)

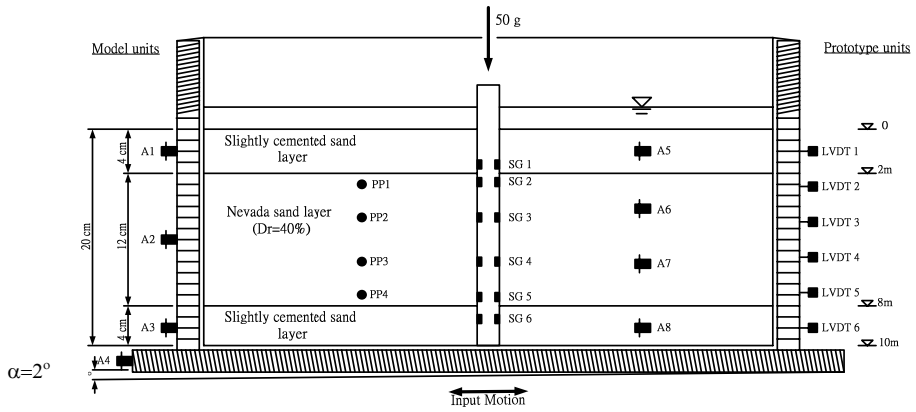

(a) Case A

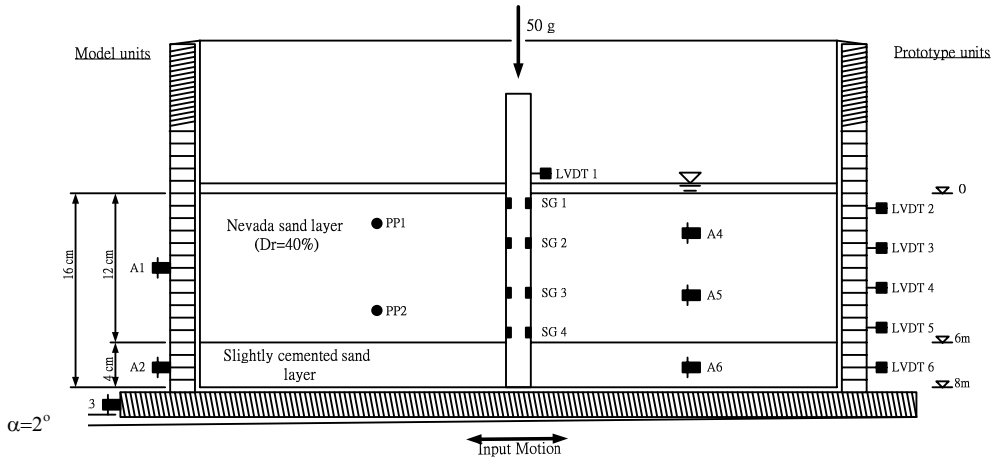

(b) Case B

Fig. 1 Centrifuge Testing Model (after Abdoun et al., 2003)

During the testing, the bottom of the box is applied with an excitation to simulate earthquake motion. The excitation has frequency of 20Hz, maximum magnitude of 0.3g, and 40 cycles. In order to simulate the effect of lateral spreading, the entire box is tilted at 4.8° .

Case B

As shown in Fig. 1(b), input motion of Case B is the same as Case A. However, the major difference is in the soil profiles. In Case B, there is no surface layer of the slightly cemented sand.

To verify the accuracy of the materials model proposed in this paper, the verification procedure includes two steps, including CYCLIC-1D simulation and the materials modeling calculation.

CYCLIC-1D Simulation

CYCLIC-1D was developed at the University of California at San Diego (Elgamal et al., 2002) to solve soil liquefaction-induced lateral spreading problems. By providing the soil properties and soil profiles, it can estimate several soil responses (e.g. acceleration, spectrum, excessive pore water pressure, etc.) under the effect of the base motion. For further information, please access http://cyclic.ucsd.edu/index.html for details.

In this step, this study uses CYCLIC-1D to simulate the acceleration and pore water pressure time histories within various depths of the prototype test, including depth of 1m, 4m, 6m, and 9m. Fig. 2(a) and Fig. 2(b) show the results of Case A; Fig.2(c) show the results of Case B. Note that the acceleration time histories in various depths of Cases A and B are the same. The data generated in this

step are implemented with the materials modeling to estimate the lateral displacement and bending moment at the corresponded depth of pile.

Materials Modeling Calculation

Combined with the results from the CYCLIC-1D, the materials model estimates the lateral displacement and the bending moment of the pile. The parameters used for the material model are given in Table 2. The excess pore pressure vs. time relations at different depths of Fig. 2 is included in Eqs. 3 and 8 in the analysis. For the Case A study, Fig. 3(a) and Fig. 3(b) show the calculation results of pile lateral displacement and bending moment, respectively. Fig. 3(c) and Fig. 3(d) show the parametric study results of bending moment of pile with or without pore water pressure consideration at various time steps and at various ground inclination angles, respectively. In general, due to the soil liquefaction effect at the middle layer, the lateral movement occurs in the top and middle layer. However, the bottom layer with non-liquefiable soils remains relatively intact. This action of lateral movement produces force on the pile, which also carries the upper part of the pile to move with the soil, while the lower part of the pile remains relatively unmovable. This phenomenon produces large bending moment concentrating at the boundary between the middle liquefied layer and the bottom non-liquefied layer.

In Case B, Fig. 4(a) and Fig. 4(b) show the calculation results of pile lateral displacement and bending moment, respectively. Fig. 4(c) shows the bending moment of pile at various inclination angles. Unlike Case A, due to lack of surface cemented sand, the displacement and bending moment distributions are different. However, the maximum values still concentrate at the boundary between the liquefied layer and the bottom fixed layer. In comparing the actual measured data collected from the centrifuge data, all two cases show a good agreement between the calculation results and the actual measured data.

A BUILDING IN MIKAGEHOMA, JAPAN (TOKIMATSU, 2003)

A case history of 35cm diameter and 23m long pre-stressed high strength concrete piles supporting a four-story building in Mikagehama reviewed by Tokimatsu (2003) after the 1995 Kobe earthquake was also back studied via the method by Lin et al. (2005) for its possible failure mode. The moment curvature properties of the piles and other soil properties are given in Table 3. In the calculation procedure, possible concrete cracking effect is also considered for when the bending moment exceeds the maximum value. Fig. 5(a) and Fig. 5(b) show the simulation of acceleration and pore water pressure time histories at various depths, respectively. Fig. 5(c) shows the bending moment of pile at various depths. Field survey showed that the piles cracked near the pile head and near the bottom of the fill, causing the building to tilt, as shown in Fig. 5(c). The predicted maximum moment locations match very well with the observed concrete crack locations of the pile.

SUMMARY AND CONCLUSIONS

The uncoupled numerical analyses model approach to simulate the single pile response under the effect of the soil liquefaction ground lateral spreading was presented in this paper. The Winkler model was used to simulate soil-structure interaction between the pile and the surrounding liquefied and non-liquefied soils. The Bouc-Wen model, which had previously been successfully used to represent static and cyclic soil properties for pile analysis (Lin et al., 2001; Badoni and Makris, 1996), was extended here to model the effects of concrete cracking on the pile performance caused by ground lateral spreads.

Two centrifuge tests produced by Abdoun et al. (2003) and one real field case (Tokimatsu, 2003) were used to verify the proposed model. The CYCLIC-1D (developed at the University of California at San Diego) was used to generate the acceleration and excessive pore water pressure time histories during the soil liquefaction-induced lateral spreading event. Finally, the entire uncoupled numerical analyses approach was combined with the results of the CYCLIC-1D and the Winkler model to estimate the

lateral displacement and bending moment of the single pile under the effect of lateral spreading force. The results showed a good agreement between the measured and calculated lateral displacement and bending moment of pile.

ACKNOWLEDGEMENT

This study was supported by the National Science Council and MOTC, Taiwan, under grant number NSC 92-2211-E-019-007 and MOTC-STAO-94-01, respectively. The authors hereby express their gratitude for this support.

REFERENCES

Abdoun, T., Dobry, R., O'Rourke, T. D., and Goh, S. H. (2003). "Pile response to lateral spreads: centrifuge modeling," *Journal of Geotechnical and Geoenvironmental Engineering*, ASCE, 129(10), 869-878.

Badoni, D. and Makris, N. (1996). "Nonlinear response of single piles under lateral inertial and seismic loads." *Soil Dynamics and Earthquake Engineering*, 15, 29-43.

Badoni, D. (1997). "Nonlinear response of pile foundation-superstructure systems Dissertation Department of Civil Engineering." *University of Notre Dame, Indiana*, USA.

Bhattacharya, S., Madabhushi, S.P.G., and Bolton, M.D. (2004). "An alternative mechanism of pile failure in liquefiable deposits during earthquakes." *Geotechnique*, 54(3), 203-213.

Elgamal, A., Yang, Z., Parra, E. and Ragheb, A. (2002). Cyclic 1D-*An internet-based nonlinear finite element program for execution of one-dimensional site amplification and liquefaction simulations*, University of California at San Diego, http://cyclic.ucsd.edu/index.html for details.

Hamada M. (1992). "Large Ground Deformations and Their Effects on Lifelines: 1964 Niigata Earthquake in Case Studies of Liquefaction and Lifeline Performance During Past Earthquakes." *Japanese Case Studies, Technical Report*, NCEER-92-0001, NCEER, Buffalo, NY, USA, Vol. (1), 3.1-3.123.

Hwang, J.H., Yang, C.W., Chen, C.H. (2003). "Investigations on soil liquefaction during the Chi-Chi earthquake." *Soils and Foundations*, 43(6), 107-123.

Japanese Road Association (1996). "Specifications for highway bridges", *Part V. Seismic Design.*

Kagawa, T., Taji, Y., Sato, M., and, Minowa, C. (1992) "Soil-Pile-Structure Interaction in Liquefying Sand from Large-Scale Shaking-Table Tests and Centrifuge Tests" *Analysis and Design For Soil-Pile-Structure Inter Actions*, 69-84.

Lin, S.S., Liao, J.C., Yang, T.S., and Juang, C.H. (2001). "Nonlinear response of single concrete piles." *Geotechnical Engineering Journal*, 32(3), 165-175.

Lin, S.S., Liao, J.C., Liang, T.T., and Juang, C.H. (2002). "Use of Bouc-Wen model for seismic analysis of concrete piles." *in Deep Foundations 2002*, GSP 116, ASCE, 372-384.

Lin, S.S., Tseng, Y.J., Chiang, C.C., and Hung, C.L. (2005) "Damage of Piles Caused by Lateral Spreading- Back Study of Three Cases" in *Seismic Performance and Simulation of Pile Foundations in Liquefied and Laterally Spreading Ground*, GSP No. 145, ASCE, 121-133.

Meyersohn, W.D. (1994). "Pile response to liquefaction-induced lateral spread." *Doctor's dissertation.*, Cornell University, USA.

Tokimatsu, K., Oh-oka, H., Satake, K., Shamoto, Y., and Asaka, Y. (1998). "Effects of Lateral Ground Movements on Failure Pathenns of Piles in the 1995 Hygoken-Nambu Earthquake." *Geotechnical Earthquake Engineering and Soil Dynamics*, Vol. (3), 1175-1186.

Tokimatsu, K. (2003). "Behavior and design of pile foundations subjected to earthquakes." *Keynote Speech, 12th Asia Regional Conference on Soil Mechanics and Geotechnical Engineering*, Singapore, Vol. (2), 1065-1096.

Wen, Y.K. (1985). "response and damage of hysteretic systems under random excitation." *Proceedings of 4th International Conference on Structural Safety and reliability*, Vol. (1), 291-300.

Table 1 Soil material properties for Centrifuge Testing Model
(after Abdoun et al., 2003)

Nevada Sand	Relative Density, D_r(%)	40
	D_{10}(mm)	0.09
	D_{50}(mm)	0.15
	Specific Gravity, G_s	2.67
	Max. Void Ratio, e_{max}	0.887
	Min. Void Ratio, e_{min}	0.511
	Max. Dry Unit Wet., r_{dmax} (kN/m$^{3)}$	17.33
	Min. Dry Unit Wet.,r_{dmin} (kN/m^3)	13.87
	Permeability at 1g for *Dr*= 40% (m/s)	6.6×10^{-5}
Cemented sand	ϕ (deg.)	34.5
	C (kPa)	5

Table 2 Parameters used for the Uncoupled Analysis Model

Parameter		Centrifuge Testing	A Building in Mikagehoma
Shape Parameters of Hysteretic Loop	A	4.1	3
	β	0.09	0.5
	γ	0.09	0.5
	n	1.0	1.0
Nonlinear Hysteretic Parameter, μ		6.0	3
Frequency, ω (1/sec)		2.0	1.6
Shape Parameters of Moment-Curvature Hysteretic Loop	A_M	8	8
	B	65	1
Yielding Stiffness Parameter, α		0.95	0.3

Table 3 Material properties used for the Building in Mikagehoma, Japan (Tokimatsu, 2003)

Back studied case							
Pile		*Soil*					
E_pI_p (kN-m^2)	5000	Upper Non-liquefied layer		Middle(or upper) liquefied layer		Bottom non-liquefied layer	
M_{cr} (kN-m)	12	depth (m)	0.0-1.5	depth (m)	1.5-14.0	depth (m)	14.0-23.0
M_y (kN-m)	75	γ_s (kN/m^3)	16.5	γ_s (kN/m^3)	12.5	γ_s (kN/m^3)	18.5
M_u (kN-m)	100	ϕ (deg.)	32	ϕ (deg.)	25	ϕ (deg.)	40

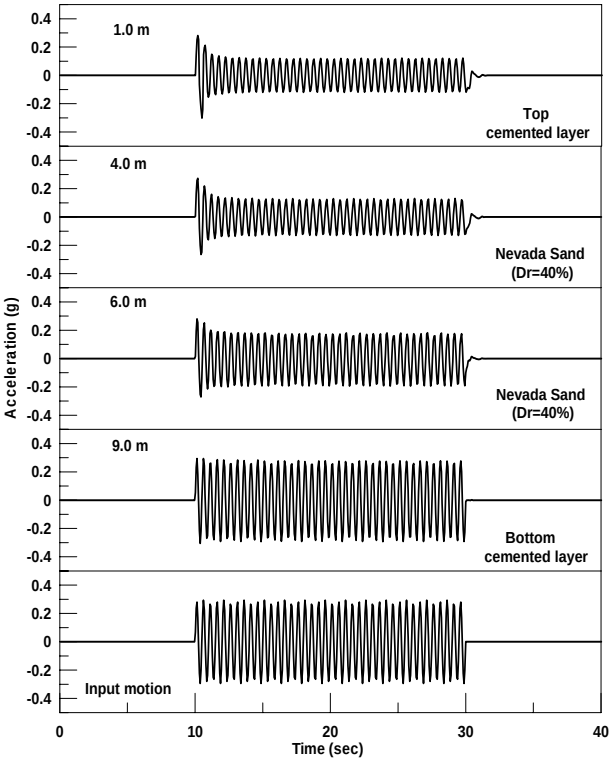

(a) acceleration time histories

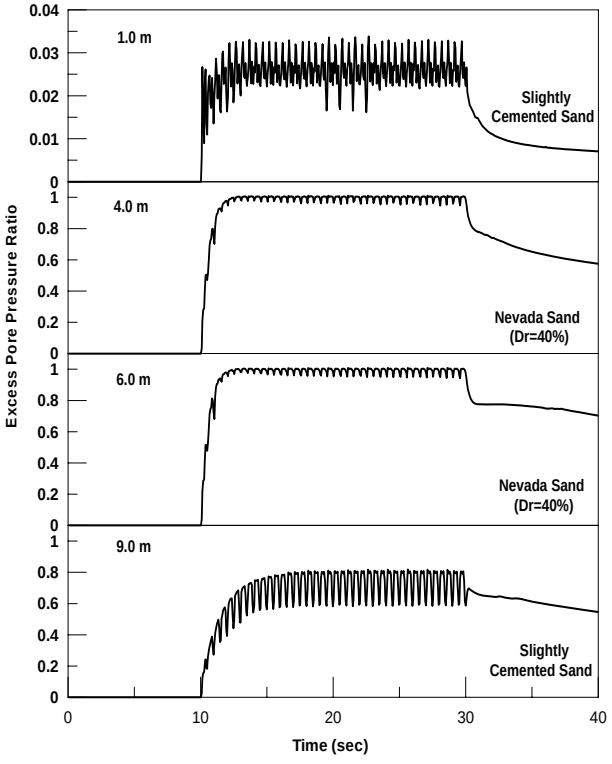

(b) pore water pressure time histories(Case A)

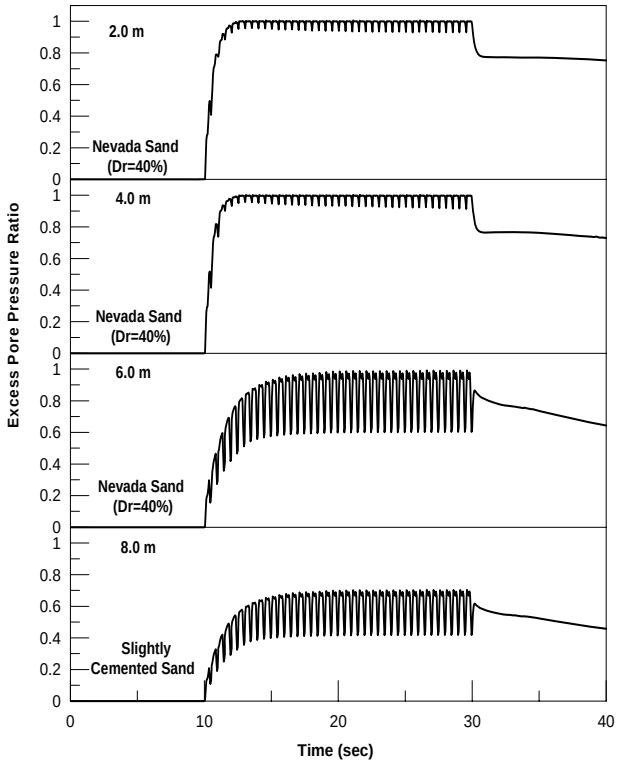

(c) pore water pressure time histories(Case B)

Fig. 2 CYCLIC-1D simulation

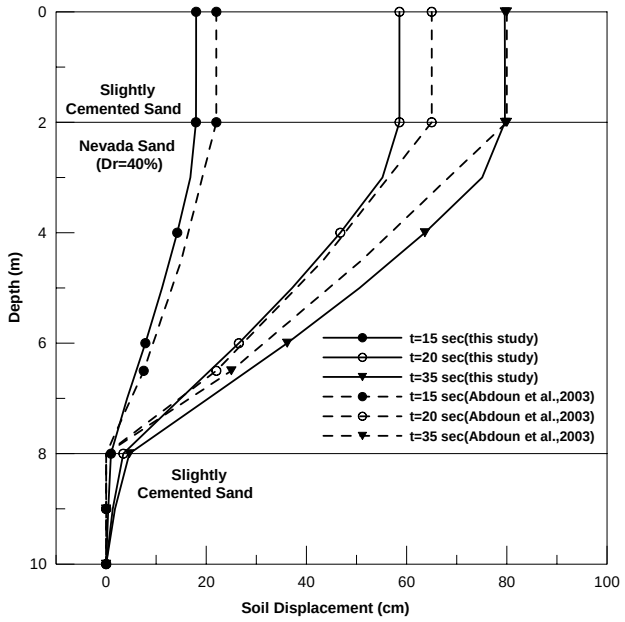

(a) lateral displacement of prototype pile at various time steps

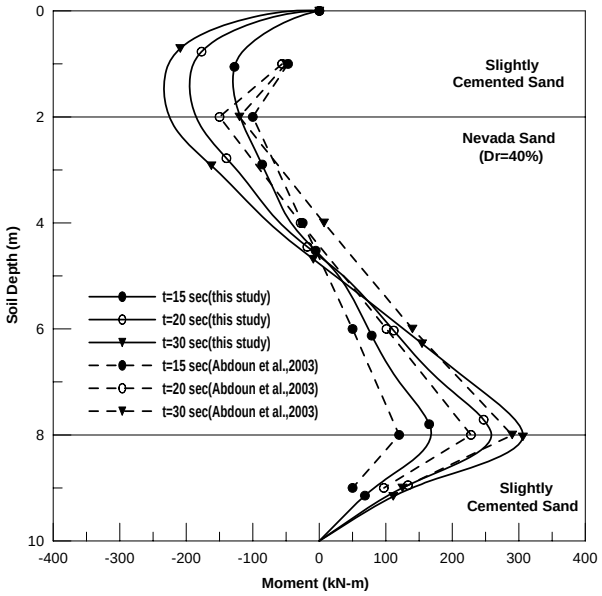

(b) bending moment of prototype pile at various time steps of Case A

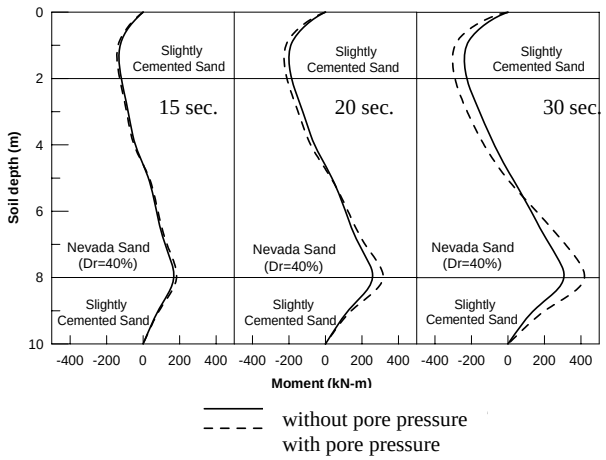

(c) bending moment of prototype pile with and without pore water pressure

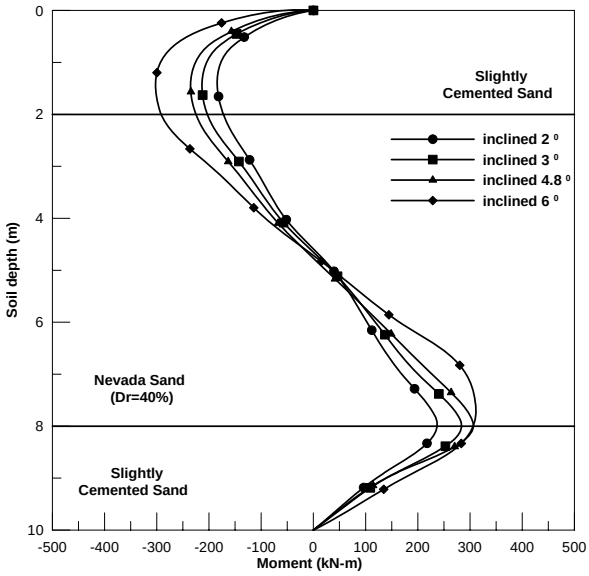

(d) bending moment of prototype pile of at various slope inclinations

Fig. 3 Calculation results of Case A

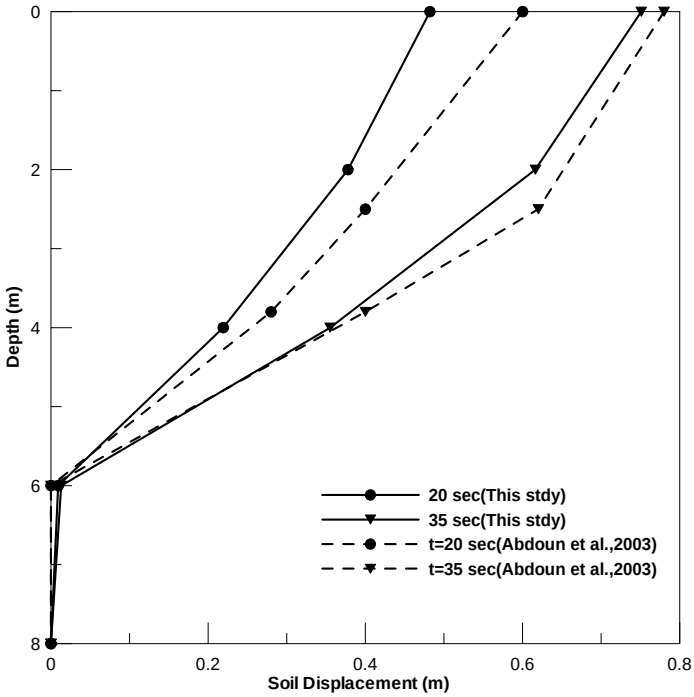

(a) lateral displacement of prototype pile at various time steps

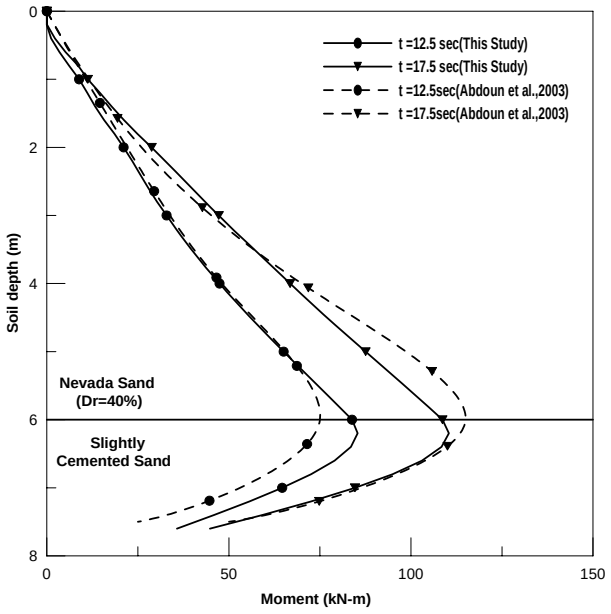

(b) bending moment of prototype pile at various time steps

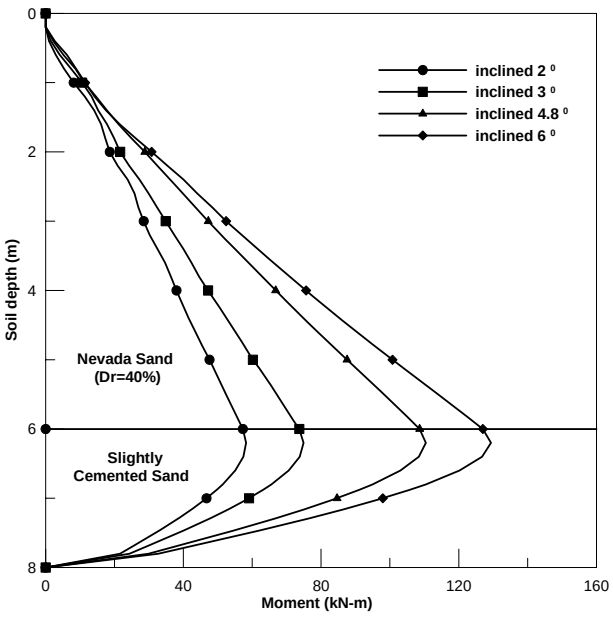

(c) bending moment of prototype pile at various slope inclinations

Fig. 4 Calculation results of Case B

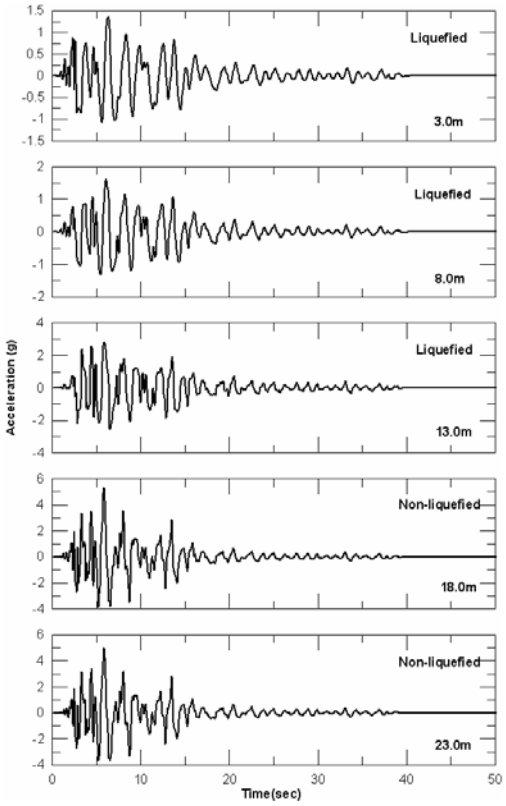

(a) simulations of acceleration time history within various depth

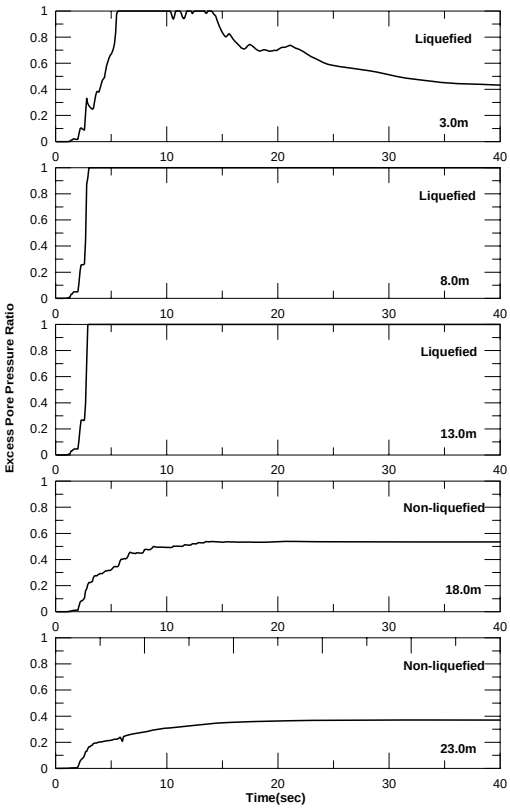

(b) simulations of pore water pressure time history within various depth

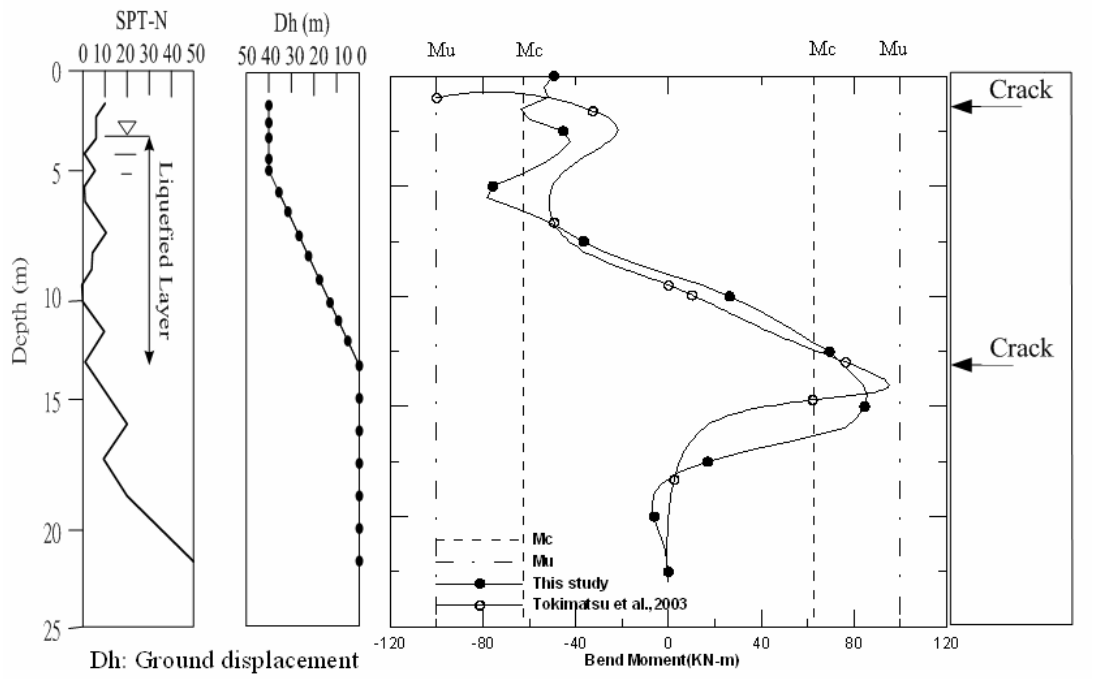

(c) bending moment of pile

Fig. 5 Calculation results of building in Mikagehoma